Stability of waves in multi-component DNLS system

Stability of Waves in Multi-component DNLS system

V. M. Rothos[†*] and P.G. Kevrekidis[††],

[†] Department of Mathematics, Physics Computational Sciences,
Faculty of Technology, Aristotle University of Thessaloniki, Thessaloniki 54124 Greece

[††] Department of Mathematics and Statistics, University of Massachusetts Amherst, MA 01003-4515 USA

February 8, 2008

Abstract

In this work, we systematically generalize the Evans function methodology to address vector systems of discrete equations. We physically motivate and mathematically use as our case example a vector form of the discrete nonlinear Schrödinger equation with both nonlinear and linear couplings between the components. The Evans function allows us to qualitatively predict the stability of the nonlinear waves under the relevant perturbations and to quantitatively examine the dependence of the corresponding point spectrum eigenvalues on the system parameters. These analytical predictions are subsequently corroborated by numerical computations.

2000 MSC 34C, 37K, 39

PACS 0230K, 0240V, 0545

[*] On leave: Department of Applied Mathematics, University of Crete, Heraklio, GR71409 Greece

Contents

1 Introduction

In the last few years, the study of solitary waves in multi-component systems has drawn a large focus of attention both in the physics of Bose-Einstein condensates [1, 2, 3, 4, 5, 6, 7], and in that of nonlinear optical fiber and waveguide arrays [8, 9].

In the case of BEC dynamics, if the condensates are in a deep optical lattice, then their dynamics can be described by a discrete nonlinear Schrödinger (DNLS) equation [10, 11, 12]. Multi-species condensates can arise, in this setting, as mixtures of different spin states in ^{87}Rb [13, 14] and ^{23}Na [15] condensates. Furthermore, theoretical studies have discussed the possibilities of mixtures between different atomic species, such as Na–Rb [16, 17], K–Rb [18, 19], Cs–Rb [20] and Li–Rb [21]. A two-species BEC, in fact in a ^{41}K–^{87}Rb mixture, has been recently reported [22]; finally, a mixture of ^{7}Li and ^{133}Cs was also experimentally investigated [23] (albeit in a non-condensed state). In the above contexts, the relevant theoretical models, in the presence of an optical lattice trapping [4], consists of one DNLS equation per atomic species. These equations are coupled by nonlinear cross-phase modulation (XPM); however, linear coupling terms can also be applied to the description of BEC dynamics in this mean-field approximation. The nonlinear interaction between the components is generated by (inter-species) atomic collisions, while linear coupling may be readily induced by an external microwave or radio-frequency field which induces Rabi [24] or Josephson [25] oscillations between populations of the two states.

Numerous issues have been considered, especially in the continuum (i.e., non-lattice) counterpart of the above framework. Among them, are ground-state solutions [16, 26, 27], small-amplitude excitations [17, 28], formation of *domain walls* (DWs) between immiscible species [29, 30, 31, 32], bound states of dark-bright [33] and dark-dark [34], dark-gray, bright-gray, bright-antidark and dark-antidark [35] complexes of solitary waves, spatially periodic states [36] and modulated amplitude waves [37] among others.

A realization of the above discussed system is quite possible also in the setting of the coupled optical waveguides. In that case, the two species represent either two orthogonal polarizations of light, or two signals with different carrier wavelengths. In the latter case, the linear coupling can also be implemented, by twisting the waveguides or elliptically deforming them, in the case of linear or circular polarizations, respectively. In this context, strongly localized vector (two-component) discrete solitons have been identified, both in one-dimension [38, 39], as well as in two dimensions [40]. Similarly to their continuous counterparts [41], these vector solitons may have components of different types (bright, dark, or antidark). In particular, symbiotic bright-dark and dark-antidark pairs were predicted in such systems [38, 39]. Such solitary waves have also been observed experimentally, see e.g., [42].

These recent developments, on both theoretical and also experimental aspects of such multi-component systems underscore the relevance of further systematic studies of their coherent structures and, importantly, also of their stability. More specifically, in the discrete setting, the stability of solitary waves in (a single-component) DNLS and related models was addressed in [43]. However, to the best of our knowledge, there were no works developing techniques systematically addressing the stability of waves in the context of vector discrete equations. This formulates the problem that the present study aims at addressing. In particular, we use as our starting point a vector integrable discretization of [44, 45] (see also [46] and references therein). We then include perturbations, through the inclusion of physically relevant terms, such as ones that appear in the framework of the coupled DNLS models or the linear coupling discussed above (see e.g. [24, 25]). We focus on the influence of such terms on the point spectrum eigenvalues of the linearization around the perturbed solitary waves. To monitor the latter, we generalize the Evans function methodology of [43] (see also [47] for the continuum setting) to address the vector case and obtain good agreement of the relevant predictions with the qualitative phenomenology and the quantitative dependence on (the perturbed) system parameters.

Our presentation will be structured as follows. In section 2, we are going to give the general setup and notation of the coupled equation system. In section 3, we are going to develop the Evans function for the vector case and use it to obtain the eigenvalues in the case of DNLS-like perturbations. In section 4, we are going to give the corresponding results in the presence of linear coupling. In these two sections, the analytical results will be complemented with numerical computations. Finally, in section 5, we summarize our findings and present our conclusions.

2 The CDNLS equation and Notation

We consider the case of two coupled discrete NLS (CDNLS) equations in the form

$$\begin{aligned} \mathrm{i}\dot{u}_n &= -\Delta_2 u_n - (|u_n|^2 + |v_n|^2)(u_{n+1} + u_{n-1}) - 2\varepsilon u_n(|u_n|^2 + |v_n|^2) \\ \mathrm{i}\dot{v}_n &= -\Delta_2 v_n - (|v_n|^2 + |u_n|^2)(v_{n+1} + v_{n-1}) - 2\varepsilon v_n(|v_n|^2 + |u_n|^2) \end{aligned} \tag{2.1}$$

with

$$\Delta_2 := \frac{1}{h^2}(u_{n+1} - 2u_n + u_{n-1})$$

; h is the step-size of discretization and n is the lattice site index. Our motivating physical setting stems from the consideration of coupled hyperfine states of an atomic species (such as the spin states $|1, -1>$ and $|2, 1>$ of ^{87}Rb; see [13, 14] for relevant details), examined in the presence of a quasi-one-dimensional deep optical lattice potential. A vector generalization of the derivation of [12] would establish the coupled discrete NLS model (with near-unity nonlinearity coefficients [14]) as the appropriate underlying mathematical framework. However, a starting point that is more tractable analytically is the $\varepsilon = 0$ variant of the above model of Eqs. (2.1) (i.e., the "Ablowitz-Ladik limit" [44, 45]). We therefore study first the existence and stability of discrete solitons for CDNLS equations starting from the $\varepsilon = 0$ limit and using continuation in ε small to examine the persistence of such solutions in the non-integrable limit with the onsite nonlinearity. We study analytically the stability of discrete solitons of the above coupled system for $C \equiv 1/h^2 = 1$ through the Evans method and the properties of reduced discrete dynamical system (perturbed 4-dimensional mapping). Based on the integrability of this map one can provide an analytic expression of the discrete Evans function. Concerning small perturbations of integrable CDNLS model, we wish to study the stability criteria for discrete solitons and test these predictions against numerical simulations. We note in passing that this type of discretization does have the relevant Manakov continuum limit as $h \to 0$, where the equations become

$$iu_t = -\Delta u - (1+\epsilon)\left(|u|^2 + |v|^2\right)u, \tag{2.2}$$

$$iv_t = -\Delta v - (1+\epsilon)\left(|u|^2 + |v|^2\right)v, \tag{2.3}$$

up to rescaling of the amplitudes ($u \to u\sqrt{1+\epsilon}$ and $v \to v\sqrt{1+\epsilon}$) or one of space and time (i.e., $x \to x\sqrt{1+\epsilon}$ and $t \to t(1+\epsilon)$). Notice that this particular discretization is motivated by the wide volume of work on the so-called Salerno model [48] which is also considering a mixed nonlinearity of combined local and nearest-neighbor nonlinear term.

We are interested in stationary solutions of the system of equations (2.1) and make the ansatz

$$u_n(t) = q_n \mathrm{e}^{-\mathrm{i}\omega t}, \qquad v_n(t) = p_n \mathrm{e}^{-\mathrm{i}\omega t}, \tag{2.4}$$

with a uniform rotation frequency ω. Using Equations (2.4) in Equations (2.1), we arrive at two coupled second–order difference equations

$$
\begin{aligned}
q_{n+1}+q_{n-1} &= \frac{2-\omega h^2}{1+h^2(q_n^2+p_n^2)}\,q_n-\varepsilon 2h^2 q_n\frac{(q_n^2+p_n^2)}{1+h^2(q_n^2+p_n^2)}\\
p_{n+1}+p_{n-1} &= \frac{2-\omega h^2}{1+h^2(q_n^2+p_n^2)}\,p_n-\varepsilon 2h^2 p_n\frac{(q_n^2+p_n^2)}{1+h^2(q_n^2+p_n^2)}.
\end{aligned}
\tag{2.5}
$$

For $\varepsilon=0$, we obtain the integrable standard–like map with two invariants:

$$
I_1=h^2\left[\left(q_n^2+q_{n-1}^2-2\mathrm{c}q_nq_{n-1}\right)+\left(p_n^2+p_{n-1}^2-2\mathrm{c}p_np_{n-1}\right)+h^2\,(q_n^2+p_n^2)(q_{n-1}^2+p_{n-1}^2)\right]
$$

$$
I_2=\frac{h^2}{\mathrm{c}^2}\left[q_n^2+q_{n-1}^2-2\mathrm{c}q_nq_{n-1}+p_n^2+p_{n-1}^2-2\mathrm{c}p_np_{n-1}+\frac{h^2}{\mathrm{c}}\left(q_nq_{n-1}+p_np_{n-1}\right)^2\right]
$$

where $\mathrm{c}=2-\omega h^2$.

Upon setting

$$
r_n=(q_n-q_{n-1})/h,\quad s_n=(p_n-p_{n-1})/h,
$$

the steady–state problem for CDNLS can be formulated as

$$
\begin{aligned}
q_{n+1} &= (\mathrm{c}\chi-1)q_n+r_nh+\varepsilon(\,-2h^2\,)q_n(q_n^2+p_n^2)\chi\\
r_{n+1} &= (\mathrm{c}\chi-1)\frac{q_n}{h}+r_n+\varepsilon(\,-2h\,)q_n(q_n^2+p_n^2)\chi\\
p_{n+1} &= (\mathrm{c}\chi-1)p_n+s_nh+\varepsilon(\,-2h^2\,)p_n(q_n^2+p_n^2)\chi\\
s_{n+1} &= (\mathrm{c}\chi-1)\frac{p_n}{h}+s_n+\varepsilon(\,-2h\,)p_n(q_n^2+p_n^2)\chi,
\end{aligned}
\tag{2.6}
$$

where

$$
\chi=\frac{1}{1+h^2(q_n^2+p_n^2)}.
$$

The equations (2.6) are written so that when $\varepsilon=0$, they are then exactly the steady–state problem for integrable CDNLS.

When $\varepsilon=0$ the solutions are given by

$$
\begin{aligned}
Q_n(\xi) &= \frac{\alpha_1\sinh 2W}{\sqrt{\alpha_1^2+\alpha_2^2}}\,\mathrm{sech}(\tilde{W}n+\xi),\\
P_n(\xi) &= \frac{\alpha_2\sinh 2W}{\sqrt{\alpha_1^2+\alpha_2^2}}\,\mathrm{sech}(\tilde{W}n+\xi),
\end{aligned}
\tag{2.7}
$$

with $\tilde{W}=\cosh^{-1}(\mathrm{c}/2)=2W$. For small h, $\tilde{W}\approx\sqrt{-\omega}h$. Note that these solutions precisely describe the stable and unstable manifolds of the fixed point $(0,0,0,0)$, and that these manifolds intersect non–transversely. This is a non–generic phenomenon for standard-like maps, and hence it is expected that the intersection, if it persists, will be transverse for $\varepsilon>0$.

Addressing the linear stability of the wave, we set $u_n=u_R+\mathrm{i}u_I, v_n=v_R+\mathrm{i}v_I$ and linearizing CDNLS about the wave, one has the linearized problem

$$
\begin{aligned}
\partial_t u_R &= -L_-u_I\\
\partial_t u_I &= L_{Q+}u_R+L_Qv_R
\end{aligned}
$$

$$\begin{aligned} \partial_t v_R &= -L_- v_I \\ \partial_t v_I &= L_P u_R + L_{P+} v_R \end{aligned} \tag{2.8}$$

Hence, the operators $L_-, L_Q, L_P, L_{Q+}, L_{P+}$ are given by

$$\begin{aligned} L_- &= \Delta_2 + \omega + (Q_n^2 + P_n^2)(\mathrm{e}^{\partial} + \mathrm{e}^{-\partial}) \\ L_{Q+} &= \Delta_2 + \omega + 2(Q_{n+1} + Q_{n-1})Q_n + (Q_n^2 + P_n^2)(\mathrm{e}^{\partial} + \mathrm{e}^{-\partial}) \\ L_Q &= 2P_n(Q_{n+1} + Q_{n-1}) \\ L_{P+} &= \Delta_2 + \omega + 2(P_{n+1} + P_{n-1})P_n + (Q_n^2 + P_n^2)(\mathrm{e}^{\partial} + \mathrm{e}^{-\partial}) \\ L_P &= 2Q_n(P_{n+1} + P_{n-1}) \end{aligned} \tag{2.9}$$

where $\mathrm{e}^{\pm\partial} u_n = u_{n\pm 1}$. Upon setting

$$\mathbf{L} = \begin{pmatrix} 0 & -L_- & 0 & 0 \\ L_{Q+} & 0 & L_Q & 0 \\ 0 & 0 & 0 & -L_- \\ L_P & 0 & L_{P+} & 0 \end{pmatrix}$$

it is not difficult to check that

$$\mathbf{L}\begin{pmatrix} \partial_\omega Q_n \\ 0 \\ \partial_\omega P_n \\ 0 \end{pmatrix} = \begin{pmatrix} 0 \\ Q_n \\ 0 \\ P_n \end{pmatrix}, \qquad \mathbf{L}\begin{pmatrix} 0 \\ Q_n^c \\ 0 \\ P_n^c \end{pmatrix} = \begin{pmatrix} \partial_\xi Q_n \\ 0 \\ \partial_\xi P_n \\ 0 \end{pmatrix}.$$

Q_n^c, P_n^c satisfy the condition

$$\lim_{h\to 0^+} \begin{pmatrix} Q_n^c \\ P_n^c \end{pmatrix} = -\frac{1}{2}x \begin{pmatrix} Q(x) \\ P(x) \end{pmatrix},$$

where $Q(x), P(x)$ are the continuum limit of $Q_n(\xi), P_n(\xi)$. The eigenvalue at $\lambda = 0$ has algebraic multiplicity six.

3 Evans Function and stability

We rewrite the eigenvalue problem $(\mathbf{L} - \lambda)\mathbf{u} = 0$ as a system of difference equations

$$Y_{n+1} = \mathbf{A}(\lambda, n) Y_n \tag{3.1}$$

It is known that there exist solution sets $\mathbf{Y}_n^1, \mathbf{Y}_n^2, \mathbf{Y}_n^3$ and $\mathbf{Y}_n^4, \mathbf{Y}_n^5, \mathbf{Y}_n^6$ to equation (3.1) such that $\left|\mathbf{Y}_n^i\right| \to 0$ exponentially fast as $n \to -\infty$ for $i = 1, 2, 3$ and $\left|\mathbf{Y}_n^i\right| \to 0$ exponentially fast as $n \to \infty$ for $i = 4, 5, 6$.

The Evans function associated with (3.1) is given by

$$E(\lambda) = (\mathbf{Y}_n^- \wedge \mathbf{Y}_n^+) / \prod_{j=0}^{n-1} \det(\mathbf{A}(\lambda, j))$$

satisfies the following properties [43]: $E(\lambda)$ is analytic in λ, $E(\lambda) = 0$ iff equation (3.1) has a bounded solution and the order of the zero is equal to the algebraic multiplicity of the eigenvalue.

The adjoint problem associated with equation (3.1) is

$$\mathbf{Z}_{n+1} = [\mathbf{A}(\lambda, n)^{-1}]^* \mathbf{Z}_n \tag{3.2}$$

and its solution satisfies:

$$\mathbf{Y}_n^i \cdot \mathbf{Z}_n^j = \delta_{ij} \quad i, j = 1, 2, 3, 4, 5, 6.$$

Assuming that $E(\lambda) \neq 0$, these solutions furthermore have the property $\left|\mathbf{Z}_n^i\right| \to 0$ exponentially fast as $n \to \infty$ for $i = 1, 2, 3$ and $\left|\mathbf{Z}_n^i\right| \to 0$ exponentially fast as $n \to -\infty$ for $i = 4, 5, 6$.

For the particular problem of CDNLS, we obtain the linearized system (3.1) with

$$\mathbf{A}(\lambda, n) = \begin{pmatrix} \gamma_Q & \lambda\alpha & h & 0 & -L_P\alpha & 0 & 0 & 0 \\ -\lambda\alpha & (\beta\alpha - 1) & 0 & h & 0 & 0 & 0 & 0 \\ \gamma_Q - 1/h & \lambda\alpha/h & 1 & 0 & -L_P\alpha/h & 0 & 0 & 0 \\ -\lambda\alpha/h & (\beta\alpha - 2)/h & 0 & 1 & 0 & 0 & 0 & 0 \\ -L_Q\alpha & 0 & 0 & 0 & \gamma_P & \lambda\alpha & h & 0 \\ 0 & 0 & 0 & 0 & -\lambda\alpha & (\beta\alpha - 1) & 0 & h \\ -L_Q\alpha/h & 0 & 0 & 0 & \gamma_P - 1/h & \lambda\alpha/h & 1 & 0 \\ 0 & 0 & 0 & 0 & -\lambda\alpha/h & (\beta\alpha - 2) & 0 & 1 \end{pmatrix} \tag{3.3}$$

where

$$\alpha = \left(\frac{1}{h^2} + (P_n^2 + Q_n^2)\right)^{-1}, \quad \beta = \frac{2}{h^2} - \omega,$$

$$\gamma_Q = \alpha(\beta - 2Q_n(Q_{n+1} + Q_{n-1}) - 1), \quad \gamma_P = \alpha(\beta - 2P_n(P_{n+1} + P_{n-1}) - 1).$$

The solutions of (3.1) about $\lambda = 0$ are the following

$$\begin{aligned} \mathbf{Y}_n^{1,-}(0) = \mathbf{Y}_n^{1,+}(0) &= \left[\partial_\xi Q_n, 0, \partial_\xi(Q_n - Q_{n-1})/h, 0, \partial_\xi P_n, 0, \partial_\xi(P_n - P_{n-1})/h, 0\right]^\top \\ \mathbf{Y}_n^{2,-}(0) = \mathbf{Y}_n^{2,+}(0) &= \left[0, Q_n, 0, (Q_n - Q_{n-1})/h, 0, 0, 0, 0\right]^\top \\ \mathbf{Y}_n^{3,-}(0) = \mathbf{Y}_n^{3,+}(0) &= \left[0, 0, 0, 0, P_n, 0, (P_n - P_{n-1})/h, 0\right]^\top \end{aligned} \tag{3.4}$$

Furthermore, define the relevant adjoint solutions as

$$\begin{aligned} \mathbf{Z}_n^1 &= \left[\partial_\xi(Q_{n-1} - Q_n)/h, 0, \partial_\xi Q_n, 0, \partial_\xi(P_{n-1} - P_n)/h, 0, \partial_\xi P_n, 0\right]^\top \\ \mathbf{Z}_n^2 &= \left[0, (Q_{n-1} - Q_n)/h, 0, Q_n, 0, 0, 0, 0, 0\right]^\top \\ \mathbf{Z}_n^3 &= \left[0, 0, 0, 0, (P_{n-1} - P_n)/h, 0, P_n, 0\right]^\top. \end{aligned} \tag{3.5}$$

Finally for the problem $\mathbf{Y}_n = \mathbf{A}(0, n)\mathbf{Y}$ define the solutions:

$$u_n^1 = \mathbf{Y}_n^{1,-}(0), \quad u_n^2 = \mathbf{Y}_n^{2,-}(0), \quad u_n^3 = \mathbf{Y}_n^{3,-}(0)$$

and let u_n^4, u_n^5 and u_n^6 satisfy the relations

$$u_n^4 \cdot \mathbf{Z}_n^1 = 0, \quad u_n^5 \cdot \mathbf{Z}_n^1 = 1, \quad u_n^6 \cdot \mathbf{Z}_n^1 = 0$$

$$u_n^4 \cdot \mathbf{Z}_n^2 = 1, \quad u_n^5 \cdot \mathbf{Z}_n^2 = 0, \quad u_n^6 \cdot \mathbf{Z}_n^2 = 1$$

$$u_n^4 \cdot \mathbf{Z}_n^3 = 1, \quad u_n^5 \cdot \mathbf{Z}_n^3 = 0, \quad u_n^6 \cdot \mathbf{Z}_n^3 = 0.$$

The equation of variation with respect to ε for the stable W^s and W^u manifolds is given by the non-homogeneous problem

$$\mathbf{Y}_{n+1} = \mathbf{A}(\lambda, n)\mathbf{Y}_n + \mathbf{g}_n \tag{3.6}$$

where $\{\, \mathbf{g}_n \,\}$ is a uniformly bounded sequence:

$$\mathbf{g}_n = -\varepsilon 2h(q_n^2 + p_n^2) \begin{pmatrix} hq_n \\ q_n \\ hp_n \\ p_n \end{pmatrix}.$$

The distance between stable and unstable manifolds can be calculated by

$$\partial_\varepsilon (W^s - W^u) = M(\xi, h) u_n^6, \tag{3.7}$$

where $M(\xi, h)$ is the Melnikov sum

$$M(\xi, h) = \sum_{n=-\infty}^{\infty} \mathbf{g}_n \cdot \mathbf{Z}_{n+1}$$

After the substitution of homoclinic solutions, the Melnikov function takes the form

$$M(\xi, h) = -2h \sum_{n=-\infty}^{\infty} (Q_n^2 + P_n^2)\Big(Q_n \partial_\xi Q_n + P_n \partial_\xi P_n\Big).$$

Let us consider

$$\tilde{\alpha}_1 = \frac{\alpha_1 \sinh 2W}{\sqrt{\alpha_1^2 + \alpha_2^2}}, \qquad \tilde{\alpha}_2 = \frac{\alpha_2 \sinh 2W}{\sqrt{\alpha_1^2 + \alpha_2^2}}.$$

Then, the homoclinic solutions (2.7) are given by

$$Q_n(\xi) = \tilde{\alpha}_1 Q(\xi), \quad P_n(\xi) = \tilde{a}_2 Q(\xi), \quad \text{where} \quad Q(\xi) = \operatorname{sech}(\tilde{W} n + \xi).$$

It is clear that the Melnikov sum can be rewritten as

$$M(\xi, h) = -\frac{h}{2}(\tilde{\alpha}_1^2 + \tilde{\alpha}_2^2)^2 \partial_\xi \sum_{n=-\infty}^{\infty} Q^4.$$

Using the Poisson summation formula we obtain

$$M(\xi, h) = a_\omega C_{_M} \sin(2\pi\xi/\tilde{W}) + \mathrm{O}(\mathrm{e}^{-2\pi^2/\tilde{W}}) \tag{3.8}$$

where

$$a_\omega = (\tilde{a}_1^2 + \tilde{a}_2^2)^2,$$

$$C_{_M}(\tilde{W}) = 4\frac{h}{2}\pi\Big(\frac{2\pi}{\tilde{W}}\Big)\Big(\frac{4}{3}\frac{\pi}{\tilde{W}} + \frac{4}{3}\frac{\pi^3}{\tilde{W}^3}\Big)\mathrm{e}^{-\pi^2/\tilde{W}}.$$

In order to calculate the Taylor series expansion of the Evans function about the eigenvalue $\lambda = 0$, we use the fact that $\lambda = 0$ has algebraic multiplicity six. One must therefore calculate $\partial_\lambda^6 E(0)$ (see Appendix):

$$\partial_\lambda^6 E(0) = \frac{120 \times 8}{D^2} \mathrm{B}_1 \mathrm{B}_2 \mathrm{B}_3. \tag{3.9}$$

where

$$\mathrm{B}_1 = \sum_{n=-\infty}^{\infty} \frac{\alpha}{h} \Big(Q_n^c \partial_\xi Q_n + P_n^c \partial_\xi P_n \Big) = \frac{1}{4} \int_{-\infty}^{\infty} (Q^2(x) + P^2(x))\, \mathrm{d}x + \mathrm{O}(h), \tag{3.10}$$

$$\mathrm{B}_2 = \sum_{n=-\infty}^{\infty} -\frac{\alpha}{h} Q_n \partial_\omega Q_n = -\frac{1}{2} \partial_\omega \int_{\infty}^{\infty} Q^2(x)\, \mathrm{d}x \tag{3.11}$$

and

$$\mathrm{B}_3 = \sum_{n=-\infty}^{\infty} -\frac{\alpha}{h} P_n \partial_\omega P_n = -\frac{1}{2} \partial_\omega \int_{\infty}^{\infty} P^2(x)\, \mathrm{d}x + \mathrm{O}(h). \tag{3.12}$$

Due to the fact that CDNLS system is Hamiltonian, the eigenvalues for the linearized problem will satisfy the relationship that if λ is an eigenvalue, then so is $-\lambda$ and $\pm\lambda^*$. Furthermore, for the CDNLS $[0, 0, Q_n, P_n]^\top$ remains an eigenfunction, and, in turn, $[\partial_\omega Q_n, \partial_\omega P_n, 0, 0]^\top$ remains a generalized eigenfunction; hence $\lambda = 0$ is an eigenvalue with multiplicity four in the perturbed problem. Consequently, we need to compute $\partial_\varepsilon \partial_\lambda^4 E(0)$. One can write

$$\partial_\varepsilon \partial_\lambda^4 E(0) = \Big[\partial_\varepsilon (\mathbf{Y}_n^{1,-} \wedge \mathbf{Y}_n^{1,+}) \wedge \partial_\lambda^2 (\mathbf{Y}_n^{2,-} \wedge \mathbf{Y}_n^{2,+}) \wedge \partial_\lambda^2 (\mathbf{Y}_n^{3,-} \wedge \mathbf{Y}_n^{3,+}) \wedge \mathbf{Y}_n^{1,+} \wedge \mathbf{Y}_n^{2,+} \wedge \mathbf{Y}_n^{3,+} \Big](0). \tag{3.13}$$

As above and using

$$\partial_\varepsilon (\mathbf{Y}_n^{1,-} \wedge \mathbf{Y}_n^{1,+}) = \partial_\xi M(\xi, h) u_n^6,$$

we obtain

$$\partial_\varepsilon \partial_\lambda^4 E(0) = \frac{4}{D^2} \mathrm{B}_2 \mathrm{B}_3 \partial_\xi M(\xi, h). \tag{3.14}$$

Combining the above results one has now an expansion of the Evans function about $\lambda = 0$ as

$$E(\lambda) = \mathrm{B}_2 \mathrm{B}_3 \frac{\lambda^4}{D^2} \Big[\frac{1}{6} \varepsilon \partial_\xi M(\xi, h) + \frac{4}{3} \lambda^2 \mathrm{B}_1 \Big], \tag{3.15}$$

where $M(\xi, h)$ is given by (3.8).

The following theorem can then be stated.

Theorem 1 *Consider the stability of the solitary waves associated with the CDNLS for $h > 0$ sufficiently small. The associated linear operator has four eigenvalues at $\lambda = 0$. Furthermore, there exist only six eigenvalues near $\lambda = 0$. If $\xi = 0$, then the wave is linearly stable, and the two additional eigenvalues are purely imaginary and are given to lowest order by*

$$\lambda_s^{\pm} = \pm \mathrm{i} \sqrt{\frac{\pi \varepsilon a_\omega C_M}{4 \mathrm{B}_1 \tilde{W}}}$$

whereas if $\xi = \tilde{W}/2$, then the wave is linearly unstable, and the two additional eigenvalues are real and are given to lowest order by

$$\lambda_u^{\pm} = \pm \sqrt{\frac{\pi \varepsilon a_\omega C_M}{4 \mathrm{B}_1 \tilde{W}}},$$

The predictions of Theorem 1 were numerically tested in Figs. 1 and 2 for the site-centered and inter-site centered modes numerically. The solutions were constructed for different values of ϵ, using a fixed point iteration scheme on a 100-site lattice. The starting point used was the analytically available solutions [46] at the limit of $\epsilon = 0$ (i.e., the integrable limit). Upon convergence to the exact numerical solution for finite ϵ, numerical linear stability analysis was performed to obtain the spectrum of linearization around the solitary waves. We observed that as soon as one deviates from the integrable limit, for this nonlinearly coupled case, the effective translational invariance of the discrete model is "broken" resulting in the bifurcation of the relevant pair of eigenvalues from the origin of the spectral plane. This bifurcation will occur along the imaginary axis for the site-centered mode of Fig. 1, while the eigenvalues will exit as real in the inter-site centered case of Fig. 2, in accordance with Theorem 1. Furthermore, the dependence of the eigenvalues will be essentially proportional to $\sqrt{\epsilon}$ as is quantified in the right panel of the relevant figures, which is consonant with the prediction of Theorem 1 above, according to which $\lambda \propto \epsilon^{1/2}$. On the contrary, the two phase invariances of the two components, corresponding to the respective "mass" conservation laws norm of each field are preserved by the nonlinear coupling. As a result, the relevant 2 pairs of eigenvalues at the spectral plane origin, will remain at $\lambda = 0$.

We note in passing that another implication of Theorem 1 concerns the near continuum limit behavior of the relevant eigenvalues, according to which:

$$\lambda \propto \exp\left(-\frac{\pi^2}{2\sqrt{-\omega}h}\right), \tag{3.16}$$

for small h, which is consistent with the earlier findings of [43] (see also references therein about exponentially small splittings of eigenvalues in the presence of discreteness). Hence, approaching the continuum limit (for fixed ϵ, and $h \to 0$), the relevant translational eigenvalue pair would approach $\lambda^2 = 0$, in direct analogy to its scalar case [43] (given this analogy, we do not examine this case further). In the line of this qualitative analogy (the quantitative details and relevant constants differ due to presence of two components here), Theorem 1 can be parallelized to Theorem 3.4 of [43].

A further note can be added regarding possible variations of the scattering lengths, which is relevant e.g., to our motivating example of two hyperfine states of ^{87}Rb [13, 14]. Slight deviations of the scatterings lengths from their unit values as well as possible changes of the coupling constants among the different components do not change the relevant eigenvalue count (since they do not affect the symmetries of the problem) or the over-arching stability conclusions for on-site versus inter-site modes.

4 Coupled DNLS with Linear Coupling

In this section, we consider a system of CDNLS equations with linear coupling:

$$\begin{aligned} \mathrm{i}\dot{u}_n &= -\Delta_2 u_n - (|u_n|^2 + |v_n|^2)(u_{n+1} + u_{n-1}) + \delta v_n \\ \mathrm{i}\dot{v}_n &= -\Delta_2 v_n - (|v_n|^2 + |u_n|^2)(v_{n+1} + v_{n-1}) + \delta u_n. \end{aligned} \tag{4.1}$$

We are interested in stationary solutions of the system of equations (2.1) and make the ansatz

$$u_n(t) = q_n \mathrm{e}^{-\mathrm{i}\omega t}, \qquad v_n(t) = p_n \mathrm{e}^{-\mathrm{i}\omega t}, \tag{4.2}$$

with a uniform rotation frequency ω. Upon setting

$$r_n = (q_n - q_{n-1})/h, \quad s_n = (p_n - p_{n-1})/h,$$

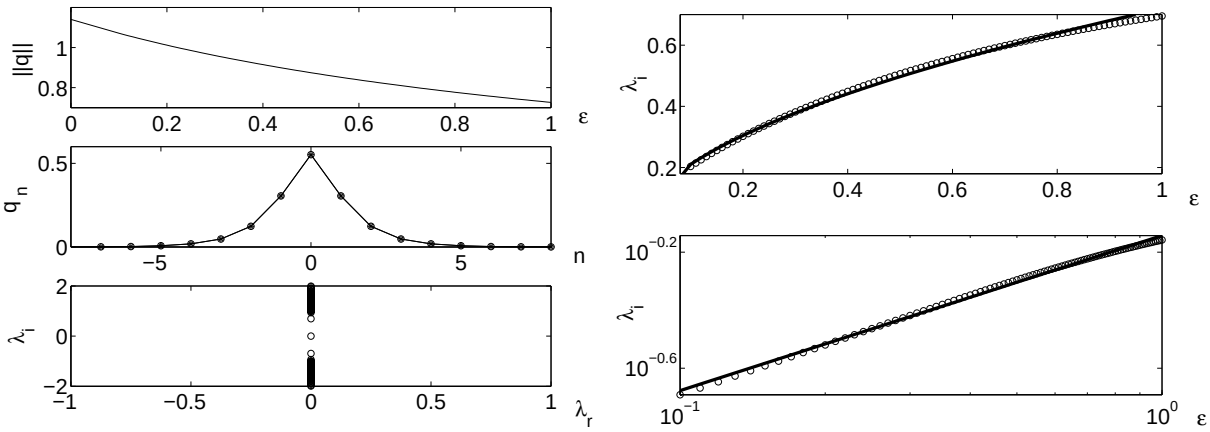

Figure 1: The left panels of the figure show the branch of stable, site-centered solitons stemming from the continuation of the integrable case of $\epsilon = 0$: the top panel shows the norm of the solution as a function of ϵ; the middle shows the discrete soliton spatial profile for $\epsilon = 1$ and the bottom panel shows the spectral plane of the linearization eigenvalues around the solution (again for $\epsilon = 1$). The right panels show the evolution of the eigenvalue bifurcating from the origin of the spectral plane (due to the breaking of the "effective" translational invariance of the integrable case. The trajectory of this imaginary eigenvalue pair is shown as a function of ϵ in linear (top panel) and log-log (bottom panel) plot. The best fit power law is shown by solid line and has the exponent $p = 0.53$.

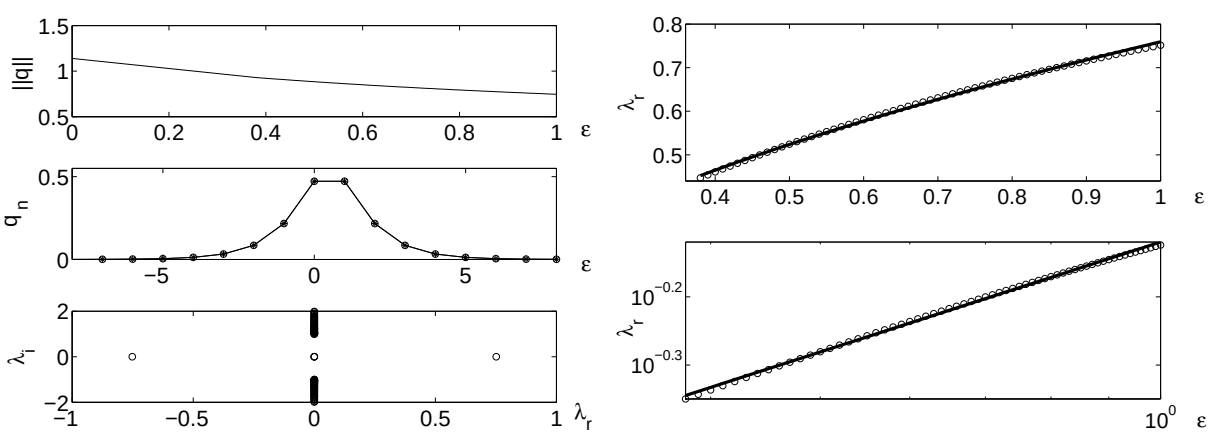

Figure 2: The same features are shown as in Fig. 1 but for the inter-site centered localized mode, where the relevant translational eigenvalue pair becomes real rendering the configuration unstable. The best fit exponent is $p = 0.54$ in the right panel showing the real eigenvalue pair as a function of ϵ.

the steady–state problem for CDNLS can be formulated as

$$\begin{aligned} q_{n+1} &= (\mathrm{c}\chi - 1)q_n + r_n h + \delta h^2 p_n \chi \\ r_{n+1} &= (\mathrm{c}\chi - 2)\frac{q_n}{h} + r_n + \delta h p_n \chi \\ p_{n+1} &= (\mathrm{c}\chi - 1)p_n + s_n h + \delta h^2 q_n \chi \\ s_{n+1} &= (\mathrm{c}\chi - 2)\frac{p_n}{h} + s_n + \delta h q_n \chi \end{aligned} \tag{4.3}$$

where

$$\mathrm{c} = 2 - \omega h^2 \quad \text{and} \quad \chi = \frac{1}{1 + h^2(q_n^2 + p_n^2)}.$$

The equations (4.3) are written so that, when $\delta = 0$, they revert to the steady–state problem for integrable CDNLS.

The equation of variation with respect to ε for the stable W^s and W^u manifolds is given (as in the CDNLS (2.1) by the non-homogeneous problem

$$\mathbf{Y}_{n+1} = \mathbf{A}(\lambda, n)\mathbf{Y}_n + \mathbf{g}_n, \tag{4.4}$$

where $\{\, \mathbf{g}_n \,\}$ is a uniformly bounded sequence:

$$\mathbf{g}_n = \delta h \begin{pmatrix} h p_n \chi \\ p_n \chi \\ h q_n \chi \\ q_n \chi. \end{pmatrix}$$

The distance between stable and unstable manifolds can be calculated by

$$\partial_\delta (W^s - W^u) = M_2(\omega, h) u_n^4. \tag{4.5}$$

$M_2(\omega, h)$ is the Melnikov sum

$$M_2(\omega, h) = \sum_{n=-\infty}^{\infty} \mathbf{g}_n \cdot \tilde{\mathbf{Z}}_{n+1},$$

where the factor χ in $\mathbf{g}$ is eliminated because we examine what happens for small h and

$$\tilde{\mathbf{Z}}_n = \Big[\, \partial_\omega (Q_{n-1} - Q_n)/h, \partial_\omega Q_n, \partial_\omega (P_{n-1} - P_n)/h, \partial_\omega P_n \,\Big]^\top$$

the second "growth mode" is obtained by solving the inhomogeneous equation.

It is clear that the Melnikov sum can be rewritten as

$$M_2(\omega, h) = h\delta\partial_\omega \sum_{n=-\infty}^{\infty} P_n Q_n = \delta\partial_\omega \int_{-\infty}^{\infty} P(x)Q(x)dx + \mathrm{O}(h),$$

where Q_n, P_n are defined in (2.7). Using the continuum limit of P and Q, one can approximate M_2 close to the continuum limit as:

$$M_2 = -\frac{\alpha_1 \alpha_2}{\alpha_1^2 + \alpha_2^2} \delta (-\omega)^{-1/2}. \tag{4.6}$$

Combining the above results one has now an expansion of Evans function about $\lambda = 0$, similarly to Eq. (3.15), involving the derivatives $\partial_\delta \partial_\lambda^4(0)$ and $\partial_\lambda^6 E(0)$, as the leading terms; the details are left to the interested reader, being quite similar to those of the previous section. One then has the following theorem:

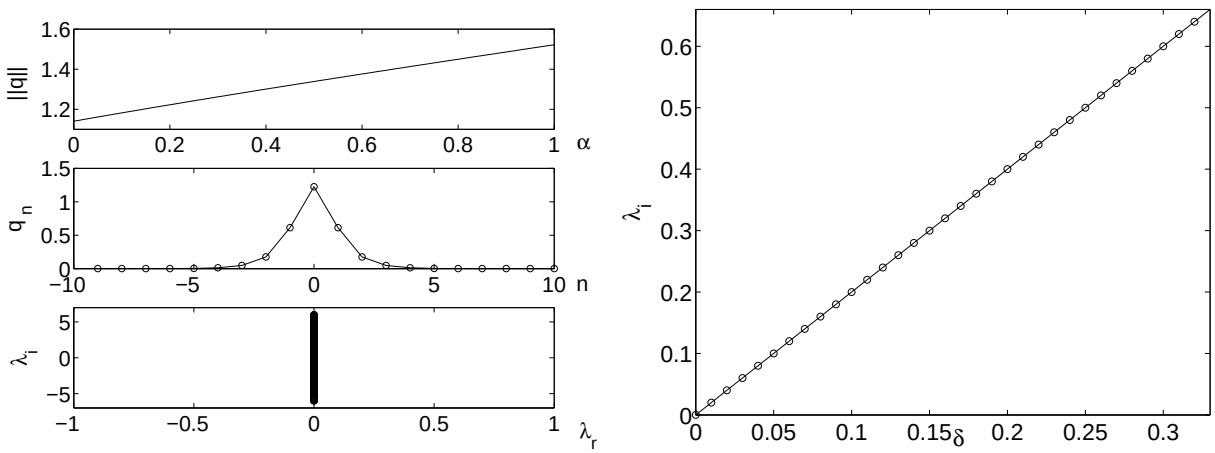

Figure 3: The left panels are similar to those of Fig. 1, but are now for the site-centered mode in the case of linear coupling between the components. The middle and bottom left panels show the field profile and the stability for the case of $\delta = 1$. The right panel shows the eigenvalue bifurcating from the origin as soon as δ becomes non-zero. The circles denote the full numerical results, while the solid line denotes the curve $\lambda_i = 2\delta$, which approximates very well the numerical result.

Theorem 2 *Consider the stability of the solitary waves associated with the CDNLS (4.1) for $h > 0$ sufficiently small. The associated linear operator has four eigenvalues at $\lambda = 0$. Furthermore, there exists an additional pair of eigenvalues near $\lambda = 0$ which are purely imaginary and directly proportional to δ.*

We have tested the above predictions numerically and have found them to be in good agreement with the computational results. In particular, the site-centered and inter-site centered modes are respectively shown in Figs. 3 and 4 for the case of linear coupling (in order to compare/contrast them with those of nonlinear coupling in Figs. 1-2). The main thing to notice in this case is that the eigenvalue bifurcation is not only linear in its dependence of the linear coupling parameter α, but is furthermore along the imaginary axis for *both* the site-centered and inter-site centered solutions. The latter implies the absence of instability in such linearly coupled cases. It is important to highlight here a key difference between the linear and nonlinear coupling case, to which this difference in stability properties can be attributed. In the latter case, examined previously, the effective translational invariance of the integrable limit was "destroyed" upon the action of the nonlinear coupling, while the relevant phase invariances remained intact. On the contrary, in the linearly coupled case, the translational invariance remains present, while one of the phase invariances is destroyed, as it is now only the sum of the squared l^2 norms that is conserved (rather than each individual one of them). As a result, the source of the bifurcation, and hence the ensuing stability behavior is different in the two cases. This is also implicitly mirrored in the similar stability behavior of the site-centered and inter-site centered modes. Finally, let us make, in passing, another important observation for the linear case. For the setting examined above with solutions identical between the two components i.e., with $q_n = p_n$, it is straightforward to note that the exact solution is analytically available for all values of the linear coupling δ, as the latter merely renormalizes W, by replacing ω with $\omega - \delta$ in the relevant expression. Furthermore, an alternative way to see that the case with the linear coupling should lead to linear dependence of the near $\lambda = 0$ eigenvalue pair as a function of δ is the following. Consider the linear transformation [49]

$$\begin{pmatrix} u_n \\ v_n \end{pmatrix} = \begin{pmatrix} \cos(\delta t) & -i\sin(\delta t) \\ -i\sin(\delta t) & \cos(\delta t) \end{pmatrix} \begin{pmatrix} \tilde{u}_n \\ \tilde{v}_n \end{pmatrix}.$$

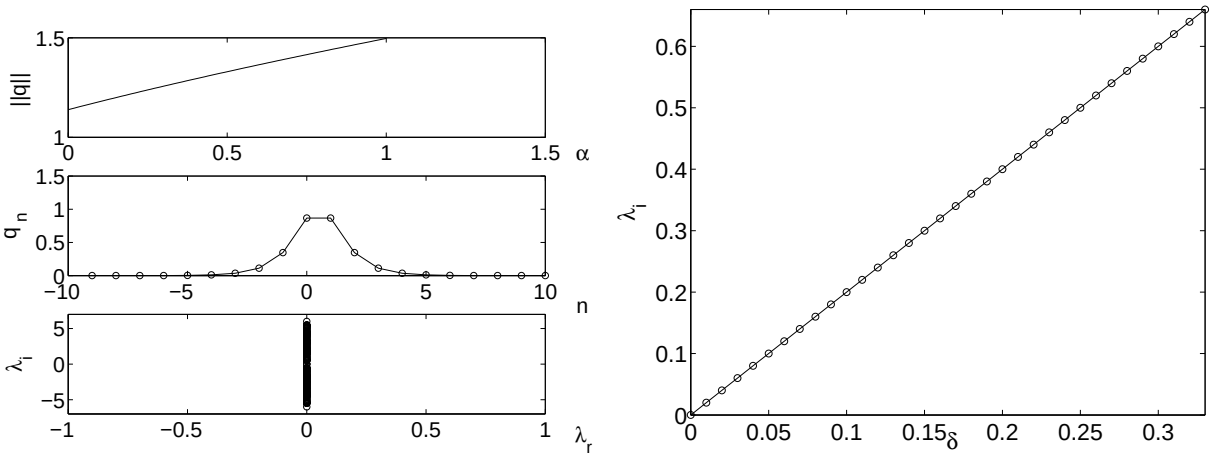

Figure 4: The same features are shown as in Fig. 3 but for the case of the inter-site centered mode. The middle and bottom left panels are for $\delta = 0.5$. The right panel shows the eigenvalue bifurcating from the origin. The circles denote the full numerical linear stability results, while the solid line denotes the curve $\lambda_i = 2\delta$.

It is interesting to observe that the equations satisfied by $\tilde{u}_n$ and $\tilde{v}_n$ are those of the *original* model i.e., *without the linear coupling*. Hence, the linear coupling can be "factored out" through this transformation, which is motivated by first-order vector systems of ordinary differential equations (and respected by our Manakov-type nonlinearity). The eigenvalues of the transformation matrix are $\exp(i\delta t)$ and $\exp(-i\delta t)$, which in turn suggests a linear dependence of the bifurcating pair of eigenvalues on δ in agreement with our numerical results of Figs. 3-4.

5 Conclusions

In conclusion, in this paper we have developed the Evans function methodology for discrete nonlinear Schrödinger equations in the vector case. We have used as our starting point the integrable discretization of [44] and have introduced nonlinear, as well as linear perturbations to it breaking different kinds of invariances. As a result, pairs of eigenvalues, corresponding respectively to these invariances (of the linearization around solitary wave solutions of the equation) have moved away from the origin of the spectral plane. These pairs have been analytically tracked via the zeros of the Evans function and have been found to yield critical information about the stability of the solutions in the non-integrable, perturbed case.

In the nonlinearly coupled case, an eigenvalue pair corresponding to translations of the solitary waves has been found to bifurcate from 0, leading to either a stable (site-centered) or unstable (inter-site centered) solution. On the other hand, in the linearly coupled case, a pair corresponding to the phase invariance of the waves has been found to bifurcate linearly from the origin. In both settings, the computed results based on numerical existence and linear stability methods have successfully corroborated the analytical predictions.

It would be interesting to extend the methodology presented herein to the, very intensely studied in recent years, context of photorefractive materials [50, 51]. In the latter case, the nonlinearity is of the saturable type (coinciding with the ones studied above for low intensities, but having very different -quasi-linear- behavior at high intensities). Such studies and the corresponding extensions to higher-dimensional settings are currently in progress and will be reported in future publications.

Acknowledgements. PGK gratefully acknowledges support from NSF-DMS-0204585, NSF-DMS-0505663, NSF-DMS-0619492 and NSF-CAREER. VMR acknowledges support from IACM-FORTH, Greece.

A Calculation of $\partial_\lambda^6 E(0)$.

Here, we calculate the $\partial_\lambda^6 E(0)$. Following Kapitula [47], [43] one has

$$\partial_\lambda^6 E(0) = 120\Big[\partial_\lambda^2(\mathbf{Y}_n^{1,-}\wedge\mathbf{Y}_n^{1,+})\wedge\partial_\lambda^2(\mathbf{Y}_n^{2,-}\wedge\mathbf{Y}_n^{2,+})\wedge\partial_\lambda^2(\mathbf{Y}_n^{3,-}\wedge\mathbf{Y}_n^{3,+})\wedge\mathbf{Y}_n^{1,+}\wedge\mathbf{Y}_n^{2,+}\wedge\mathbf{Y}_n^{3,+}\Big](0). \quad \text{(A.1)}$$

For $i = 1, 2, 3$ we have

$$\partial_\lambda^2\mathbf{Y}_{n+1}^{i,\pm}(0) = \mathbf{A}(0,n)\partial_\lambda^2\mathbf{Y}_n^{i,\pm}(0) + 2\partial_\lambda\mathbf{A}(0,n)\partial_\lambda\mathbf{Y}_n^{i,\pm}(0), \quad \text{(A.2)}$$

where

$$\begin{aligned}
\partial_\lambda\mathbf{Y}_n^{1,\pm}(0) &= \Big[0, Q_n^c, 0, (Q_n^c - Q_{n-1}^c)/h, 0, P_n^c, 0, (P_n^c - P_{n-1}^c)/h\Big]^\top \\
\partial_\lambda\mathbf{Y}_n^{2,\pm}(0) &= \Big[\partial_\omega Q_n, 0, \partial_\omega(Q_n - Q_{n-1})/h, 0, 0, 0, 0, 0\Big]^\top \\
\partial_\lambda\mathbf{Y}_n^{3,\pm}(0) &= \Big[0, 0, 0, 0, \partial_\omega P_n, 0, \partial_\omega(P_n - P_{n-1})/h, 0, \Big]^\top
\end{aligned} \quad \text{(A.3)}$$

Set $\mathbf{g}_n^i = \partial_\lambda\mathbf{A}(0,n)\partial_\lambda\mathbf{Y}_n^{i,\pm}(0)$ for $i = 1, 2, 3$. Upon using the variation of parameters to solve equation (A.2), one has that

$$\begin{aligned}
\partial_\lambda^2(\mathbf{Y}_n^{1,-}\wedge\mathbf{Y}_n^{1,+})(0) &= \frac{2}{D}\Big(u_n^6\sum_{n=-\infty}^{\infty}\mathbf{g}_n^1\cdot\mathbf{Z}_{n+1}^1 + c_1u_n^1 + c_2u_n^2 + c_3u_n^3\Big) \\
\partial_\lambda^2(\mathbf{Y}_n^{2,-}\wedge\mathbf{Y}_n^{2,+})(0) &= \frac{2}{D}\Big(u_n^5\sum_{n=-\infty}^{\infty}\mathbf{g}_n^2\cdot\mathbf{Z}_{n+1}^2 + c_4u_n^1 + c_5u_n^2 + c_6u_n^3\Big) \\
\partial_\lambda^2(\mathbf{Y}_n^{3,-}\wedge\mathbf{Y}_n^{3,+})(0) &= \frac{2}{D}\Big(u_n^4\sum_{n=-\infty}^{\infty}\mathbf{g}_n^3\cdot\mathbf{Z}_{n+1}^3 + c_7u_n^1 + c_8u_n^2 + c_9u_n^3\Big).
\end{aligned} \quad \text{(A.4)}$$

Here $c_1, \cdots, c_9$ are constants. The above equations can be simplified as follows

$$\begin{aligned}
\partial_\lambda^2(\mathbf{Y}_n^{1,-}\wedge\mathbf{Y}_n^{1,+})(0) &= \frac{2}{D}\Big(u_n^6\sum_{n=-\infty}^{\infty}\frac{\alpha}{h}\Big(Q_n^c\partial_\xi Q_n + P_n^c\partial_\xi P_n\Big) + c_1u_n^1 + c_2u_n^2 + c_3u_n^3\Big) \\
\partial_\lambda^2(\mathbf{Y}_n^{2,-}\wedge\mathbf{Y}_n^{2,+})(0) &= \frac{2}{D}\Big(u_n^5\sum_{n=-\infty}^{\infty}-\frac{\alpha}{h}Q_n\partial_\omega Q_n + c_4u_n^1 + c_5u_n^2 + c_6u_n^3\Big) \\
\partial_\lambda^2(\mathbf{Y}_n^{3,-}\wedge\mathbf{Y}_n^{3,+})(0) &= \frac{2}{D}\Big(u_n^4\sum_{n=-\infty}^{\infty}-\frac{\alpha}{h}P_n\partial_\omega P_n + c_7u_n^1 + c_8u_n^2 + c_9u_n^3\Big).
\end{aligned} \quad \text{(A.5)}$$

References

[1] F. Dalfovo, S. Giorgini, L.P. Pitaevskii, and S. Stringari, Rev. Mod. Phys. **71**, 463 (1999).

[2] C.J. Pethick and H. Smith, *Bose-Einstein Condensation in Dilute Alkali Gases*, Cambridge University Press (Cambridge, 2002).

[3] L.P. Pitaevskii and S. Stringari, *Bose-Einstein Condensation*, Clarendon Press (Oxford, 2003).

[4] F. Dalfovo, S. Giorgini, L.P. Pitaevskii, and S. Stringari, Rev. Mod. Phys. **71**, 463 (1999).

[5] P.G. Kevrekidis and D.J. Frantzeskakis, Mod. Phys. Lett. B **18**, 173 (2004).

[6] V.A. Brazhnyi and V.V. Konotop, Mod. Phys. Lett. B **18**, 627 (2004).

[7] P.G. Kevrekidis, R. Carretero-González, D.J. Frantzeskakis, and I.G. Kevrekidis, Mod. Phys. Lett. B **18**, 1481 (2004).

[8] Yu.S. Kivshar and G.P. Agrawal, *Optical solitons: from fibers to photonic crystals*, Academic Press (San Diego, 2003).

[9] B.A. Malomed, Progr. Opt. **43**, 71 (2002).

[10] A. Trombettoni and A. Smerzi, Phys. Rev. Lett. 86:2353-2356, 2001.

[11] F. Kh. Abdullaev, B. B. Baizakov, S. A. Darmanyan, V. V. Konotop, and M. Salerno, Phys. Rev. A 64:043606, 10 pages, 2001.

[12] G.L. Alfimov, P.G. Kevrekidis, V.V. Konotop and M. Salerno, Phys. Rev. E 66:046608, 5 pages, 2002.

[13] C.J. Myatt, E.A. Burt, R.W. Ghrist, E.A. Cornell, and C.E. Wieman Phys. Rev. Lett. **78**, 586 (1997).

[14] D.S. Hall, M.R. Matthews, J.R. Ensher, C.E. Wieman, and E.A. Cornell, Phys. Rev. Lett. **81**, 1539 (1998).

[15] D.M. Stamper-Kurn, M.R. Andrews, A.P. Chikkatur, S. Inouye, H.-J. Miesner, J. Stenger, and W. Ketterle, Phys. Rev. Lett. **80**, 2027 (1998).

[16] H. Pu and N.P. Bigelow, Phys. Rev. Lett. **80**, 1130 (1998).

[17] H. Pu and N.P. Bigelow, Phys. Rev. Lett. **80**, 1134 (1998).

[18] G. Ferrari, M. Inguscio, W. Jastrzebski, G. Modugno, G. Roati, and A. Simoni, Phys. Rev. Lett. **89**, 053202 (2002).

[19] A. Simoni, F. Ferlaino, G. Roati, G. Modugno, and M. Inguscio, Phys. Rev. Lett. **90**, 163202 (2003).

[20] M.J. Jamieson, H. Sarbazi-Azad, H. Ouerdane, G-H. Jeung, Y.S. Lee and W.C. Lee, J. Phys. B **36**, 1085 (2003).

[21] D. Schumayer and B. Apagyi, Phys. Rev. A **69**, 043620 (2004).

[22] G. Modugno, G. Ferrari, G. Roati, R.J. Brecha, A. Simoni, and M. Inguscio, Science **294**, 1320 (2001);
G. Modugno, M. Modugno, F. Riboli, G. Roati, and M. Inguscio, Phys. Rev. Lett. **89**, 190404 (2002).

[23] M. Mudrich, S. Kraft, K. Singer, R. Grimm, A. Mosk, and M. Weidemüller, Phys. Rev. Lett. **88**, 253001 (2002).

[24] R.J. Ballagh, K. Burnett, and T.F. Scott, Phys. Rev. Lett. **78**, 1607 (1997).

[25] P. Ohberg and S. Stenholm, Phys. Rev. A **59**, 3890 (1999); J. Williams, R. Walser, J. Cooper, E. Cornell, and M. Holland, *ibid.* **59**, R31 (1999).

[26] T.-L. Ho and V.B. Shenoy, Phys. Rev. Lett. **77**, 3276 (1996).

[27] B.D. Esry, C.H. Greene, J.P. Burke, Jr., and J.L. Bohn, Phys. Rev. Lett. **78**, 3594 (1997).

[28] Th. Busch, J.I. Cirac, V.M. Pérez-Garcia, and P. Zoller, Phys. Rev. A **56**, 2978 (1997);
R. Graham and D. Walls, Phys. Rev. A **57**, 484 (1998);
B.D. Esry and C.H. Greene, Phys. Rev. A **57**, 1265 (1998).

[29] M. Trippenbach, K. Goral, K. Rzazewski, B. Malomed, and Y.B. Band, J. Phys. B **33**, 4017 (2000).

[30] S. Coen and M. Haelterman, Phys. Rev. Lett. **87**, 140401 (2001).

[31] B.A. Malomed, H.E. Nistazakis, D.J. Frantzeskakis, and P.G. Kevrekidis, Phys. Rev. A **70**, 043616 (2004); see also Math. Comput. Simulat. **69**, 400 (2005).

[32] M.I. Merhasin, B.A. Malomed, and R. Driben, J. Phys. B **38**, 877 (2005).

[33] Th. Busch and J.R. Anglin, Phys. Rev. Lett. **87**, 010401 (2001).

[34] P. Öhberg and L. Santos, Phys. Rev. Lett. **86**, 2918 (2001).

[35] P.G. Kevrekidis, H.E. Nistazakis, D.J. Frantzeskakis, B.A. Malomed, and R. Carretero-Gonzalez, Eur. Phys. J. D **28**, 181 (2004).

[36] B. Deconinck, P.G. Kevrekidis, H.E. Nistazakis, and D.J. Frantzeskakis, Phys. Rev. A **70**, 063605 (2004).

[37] M.A. Porter, P.G. Kevrekidis and B.A. Malomed, Physica D **196**, 106 (2004).

[38] S. Darmanyan, A. Kobyakov, E. Schmidt, and F. Lederer, Phys. Rev. E **57**, 3520 (1998).

[39] A. Kobyakov, S. Darmanyan, F. Lederer, and E. Schmidt, Opt. and Quant. Elect. **30**, 795 (1998).

[40] J. Hudock, P.G. Kevrekidis, B.A. Malomed and D.N. Christodoulides, Phys. Rev. E **67**, 056618 (2003).

[41] D.N. Christodoulides and R.I. Joseph, Opt. Lett. **13**, 53 (1988); D.J. Kaup, B.A. Malomed, and R.S. Tasgal, Phys. Rev. E **48**, 3049 (1993); M. Haelterman and A. Sheppard, Phys. Rev. E **49**, 3376 (1994).

[42] J. Meier, J. Hudock, D. Christodoulides, G. Stegeman, Y. Silberberg, R. Morandotti and J.S. Aitchison, Phys. Rev. Lett. **91**, 143907 (2003).

[43] T. Kapitula and P. Kevrekidis, Nonlinearity **14**, 533 (2001).

[44] M.J. Ablowitz, Y. Ohta and A.D. Trubatch, Phys. Lett. A **253**, 287 (1999).

[45] M.J. Ablowitz, B. Prinari and A.D. Trubatch, *Discrete and Continuous Nonlinear Schrödinger Systems*, Cambridge University Press (Cambridge, 2004).

[46] T. Tsuchida, H. Ujino and M. Wadati, J. Phys. A: Math. Gen. **32**, 2239 (1999).

[47] T. Kapitula, SIAM J. Math. Anal. **30**, 273 (1999).

[48] . M. Salerno, Phys. Rev. A **46**, 6856 (1992)

[49] B. Deconinck, P.G. Kevrekidis, H.E. Nistazakis and D.J. Frantzeskakis, Phys. Rev. A **70**, 063605 (2004).

[50] J.W. Fleischer, M. Segev, N.K. Efremidis and D.N. Christodoulides, Nature **422**, 147 (2003).

[51] J.W. Fleischer, G. Bartal, O. Cohen, T. Schwartz, O. Manela, B. Freedman, M. Segev, H. Buljan and N.K. Efremidis, Opt. Express **13**, 1780 (2005).

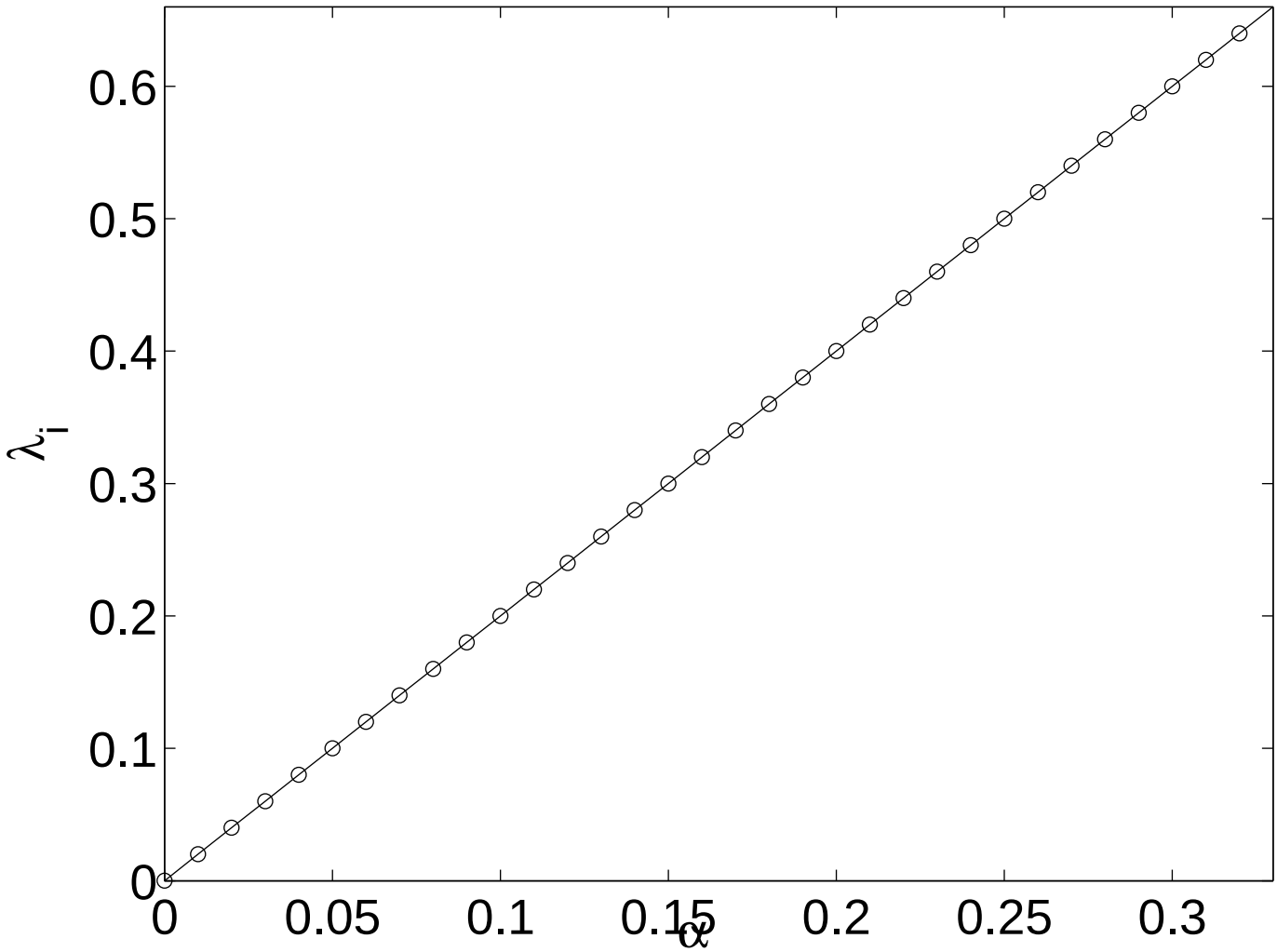
0.6
0.5
0.4
0.3
0.2
0.1
0
λ_i
0
0.05
0.1
0.15
0.2
0.25
0.3
α

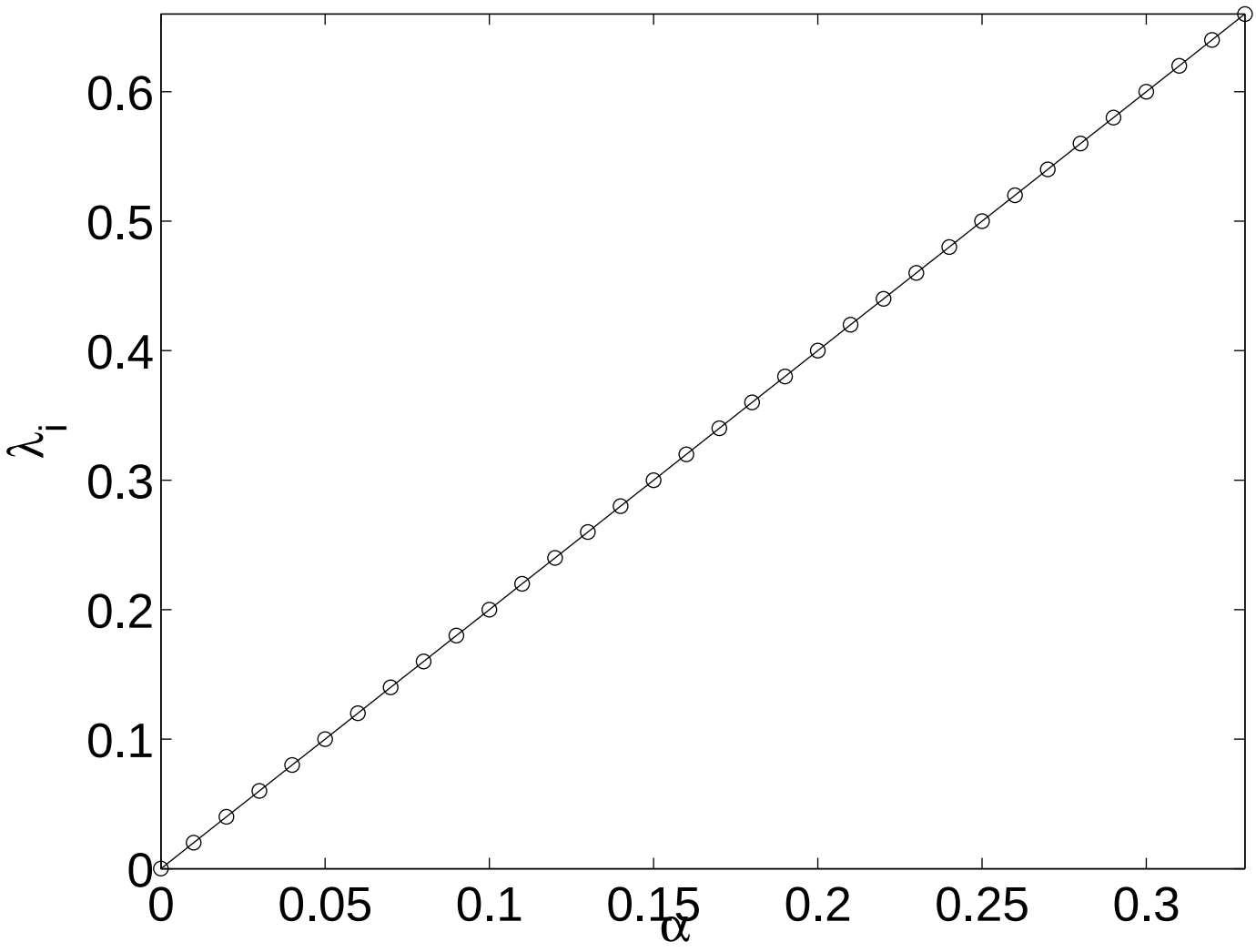
0.6
0.5
0.4
0.3
0.2
0.1
0
λ_i
0
0.05
0.1
0.15
0.2
0.25
0.3
α